

Clinical Melanoma Diagnosis with Artificial Intelligence: Insights from a Prospective Multicenter Study

Lukas Heinlein, MSc^{†1}; Roman C. Maron^{†1}, MSc; Achim Hekler^{†1}, MSc; Sarah Haggemüller¹, MSc; Christoph Wies^{1,15}, MSc; Jochen S. Utikal^{2,3,4}, MD; Friedegund Meier^{5,6}, MD; Sarah Hobelsberger⁵, MD; Frank F. Gellrich⁵, MD; Mildred Sergon⁵, MD; Axel Hauschild⁷, MD; Lars E. French^{8,9}, MD; Lucie Heinzerling^{8,11}, MD; Justin G. Schlager⁸, MD; Kamran Ghoreschi¹⁰, MD; Max Schlaak¹⁰, MD; Franz J. Hilke¹⁰, PhD; Gabriela Poch¹⁰, MD; Sören Korsing¹⁰, MD; Carola Berking¹¹, MD; Markus V. Heppt¹¹, MD; Michael Erdmann¹¹, MD; Sebastian Haferkamp¹², MD; Konstantin Drexler¹², MD; Dirk Schadendorf¹³, MD; Wiebke Sondermann¹³, MD; Matthias Goebeler¹⁴, MD; Bastian Schilling¹⁴, MD; Eva Krieghoff-Henning¹, PhD; Titus J. Brinker^{*1}, MD

1. Digital Biomarkers for Oncology Group, German Cancer Research Center (DKFZ), Heidelberg, Germany
2. Department of Dermatology, Venereology and Allergology, University Medical Center Mannheim, Ruprecht-Karl University of Heidelberg, Mannheim, Germany
3. Skin Cancer Unit, German Cancer Research Center (DKFZ), Heidelberg, Germany
4. DKFZ Hector Cancer Institute at the University Medical Center Mannheim, Mannheim, Germany
5. Department of Dermatology, Faculty of Medicine and University Hospital Carl Gustav Carus, Technische Universität Dresden, Dresden, Germany
6. Skin Cancer Center at the University Cancer Centre Dresden and National Center for Tumor Diseases, Dresden, Germany
7. Department of Dermatology, University Hospital (UKSH), Kiel, Germany

8. Department of Dermatology and Allergy, University Hospital, LMU Munich, Munich, Germany
9. Dr. Phillip Frost Department of Dermatology and Cutaneous Surgery, University of Miami, Miller School of Medicine, Miami, FL, USA
10. Department of Dermatology, Venereology and Allergology, Charité – Universitätsmedizin Berlin, Corporate member of Freie Universität Berlin and Humboldt-Universität zu Berlin, Berlin, Germany
11. Department of Dermatology, University Hospital Erlangen, Comprehensive Cancer Center Erlangen – European Metropolitan Region Nürnberg, CCC Alliance WERA, Erlangen, Germany
12. Department of Dermatology, University Hospital Regensburg, Regensburg, Germany
13. Department of Dermatology, Venereology and Allergology, University Hospital Essen, University Duisburg-Essen, Essen, Germany
14. Department of Dermatology, Venereology and Allergology, University Hospital Würzburg and National Center for Tumor Diseases (NCT) WERA Würzburg, Germany
15. Medical Faculty, University Heidelberg, Heidelberg, Germany.

†These authors contributed equally to this work.

***Correspondence to:**

Dr. Titus J. Brinker, MD

Digital Biomarkers for Oncology Group, German Cancer Research Center (DKFZ), Im

Neuenheimer Feld 223, 69120 Heidelberg, Germany

Tel.: +496221 3219304; Email: titus.brinker@dkfz.de

Keywords: dermatology, dermoscopy, melanoma, artificial intelligence, deep learning, diagnosis, diagnostic accuracy, robustness

Abstract

Early detection of melanoma, a potentially lethal type of skin cancer with high prevalence worldwide, improves patient prognosis. In retrospective studies, artificial intelligence (AI) has proven to be helpful for enhancing melanoma detection. However, there are few prospective studies confirming these promising results. Existing studies are limited by low sample sizes, too homogenous datasets, or lack of inclusion of rare melanoma subtypes, preventing a fair and thorough evaluation of AI and its generalizability, a crucial aspect for its application in the clinical setting. Therefore, we assessed “All Data are Ext” (ADAE), an established open-source ensemble algorithm for detecting melanomas, by comparing its diagnostic accuracy to that of dermatologists on a prospectively collected, external, heterogeneous test set comprising eight distinct hospitals, four different camera setups, rare melanoma subtypes, and special anatomical sites. We advanced the algorithm with real test-time augmentation (R-TTA, i.e. providing real photographs of lesions taken from multiple angles and averaging the predictions), and evaluated its generalization capabilities. Overall, the AI showed higher balanced accuracy than dermatologists (0.798, 95% confidence interval (CI) 0.779-0.814 vs. 0.781, 95% CI 0.760-0.802; $p < 0.001$), obtaining a higher sensitivity (0.921, 95% CI 0.900-0.942 vs. 0.734, 95% CI 0.701-0.770; $p < 0.001$) at the cost of a lower specificity (0.673, 95% CI 0.641-0.702 vs. 0.828, 95% CI 0.804-0.852; $p < 0.001$). As the algorithm exhibited a significant performance advantage on our heterogeneous dataset exclusively comprising melanoma-suspicious lesions, AI may offer the potential to support dermatologists particularly in diagnosing challenging cases.

Introduction

Melanoma, the leading cause of skin cancer deaths worldwide, has increased in incidence over the last few decades.¹⁻³ Early detection of this disease can reduce the size and extent of surgery as well as adverse effects of late-stage systemic therapies and is thus beneficial for patients, especially if detected pre-metastasizing.⁴ Traditionally, physicians diagnose lesions using visual inspections and dermoscopy.^{5,6} Prediction quality thereby depends on the expertise and experience of the dermatologist.⁷ Considering that the demand for such experts is increasing due to changing epidemiology, ethnographic trends, and skilled advertising,⁸ and that it is difficult to find such experts, innovative diagnostic approaches are required, especially for atypical or uncommon cases.

Recently, artificial intelligence (AI) systems for melanoma detection have emerged as a promising tool, with numerous retrospective studies reporting that AI algorithms can match or even surpass the diagnostic accuracy of experienced dermatologists in artificial settings.^{7,9-11} While the findings of these retrospective studies are undoubtedly encouraging, hinting at an improvement in patient care while reducing dermatologists' workload, a lack of prospective evaluations remains.¹² Prospective studies typically allow for more unbiased, complete and tailored evaluations, but the few existing prospective analyses of AI-based melanoma detection suffer from limitations such as a single-center design and a relatively small number of lesion samples, particularly with respect to rare melanoma subtypes.¹³⁻¹⁵

In this study, we address these limitations, thereby taking a substantial step towards comprehensive, prospective evaluations of AI-based melanoma detection, by evaluating the open source AI algorithm "All Data Are Ext"¹⁶ (ADAE) on a novel heterogeneous dataset. ADAE is a binary melanoma classifier and ranked first in the Society for Imaging Informatics in Medicine (SIIM) and International Skin Image Collaboration's (ISIC) challenge 2020.¹⁷ The dataset we introduce is heterogenous and shows substantial domain diversity. We ensure a

broad representation of potential real-life clinical and technical settings by using a multicenter design involving eight German university hospitals as well as four distinct hardware configurations. In addition, we demonstrate a strong performance of the algorithm on difficult-to-diagnose lesions, which suggests integrating AI as a supportive tool for dermatologists in diagnosing particularly challenging cases.

Results

Patient characteristics

Our dataset comprises images of a total of 1910 skin lesions that were clinically suspected to be melanoma from 1716 patients at eight German university hospitals collected between April 2021 and March 2023 (for detailed patient characteristics, see **Table 1**). The patients' age at diagnosis ranged from 18 to 96 years, with a median age of 62 years. While all skin types are present in the study population, Fitzpatrick skin types II and III are most prevalent, whereas types V and VI are less frequent.

Lesion characteristics

The dataset consists of 750 melanomas (including rare subtypes such as spitzoid or desmoplastic melanomas), 885 nevi and 275 other diagnoses (for detailed lesion characteristics, see **Table 2**). Additional information about the diagnosis, such as the exact subtype (see **Table 4**) and the self-assessed dermatologists' confidence in their diagnosis (on a scale from 1 - low confidence to 5 - high confidence), were collected. Furthermore, the lesion size and location were recorded. The lesions were collected from eight different university hospitals (i.e., the data source) with four distinct technical setups (i.e., hardware configurations, a certain combination of camera and dermatoscope that were used to capture the images, see **Supplementary Methods**), thus ensuring domain diversity.

ADAE outperforms dermatologists in balanced accuracy and sensitivity

To assess the performance of AI algorithms in diagnosing suspected melanoma lesions in prospectively acquired data, we compared the prediction quality of ADAE to that of dermatologists recorded within physical patient examinations. This assessment is based primarily on balanced accuracy, and secondarily on sensitivity and specificity. P-values smaller than 0.05 are considered statistically significant and are determined using a pairwise two-sided Wilcoxon signed-rank test. The algorithm was enhanced by providing multiple real

images per lesion in the form of so-called real test-time augmentation (R-TTA)¹⁸ (see also **Supplementary Figs. 6 and 7**). These images were first predicted individually to be melanoma or non-melanoma (including basal and spinal cell carcinoma, dermatofibroma, keratosis, nevus, vascular lesions), and ultimately aggregated to one final prediction for the respective lesion. The performance was measured using histopathological labels diagnosed by experienced pathologists as ground truth.

Overall, at the predetermined 85% sensitivity threshold (see **Methods/Model Training and Testing**), ADAE showed a higher balanced accuracy than dermatologists originally diagnosing the lesions (ADAE: 0.798, 95% confidence interval (CI) 0.779-0.814 vs. dermatologists: 0.781, 95% CI 0.760-0.802; $p < 0.001$) with significantly higher sensitivity (0.922, 95% CI 0.900-0.942 vs. 0.734, 95% CI 0.701-0.770; $p < 0.001$), but significantly lower specificity (0.673, 95% CI 0.641-0.702 vs. 0.828, 95% CI 0.804-0.852; $p < 0.001$). For the test set results, see **Table 3** and for differences stratified by domains, see **Supplementary Fig. 1-4**. In total, ADAE detected 602 of 653 melanomas (0.922 sensitivity), while dermatologists detected 479 of 653 (0.734 sensitivity), respectively (for the individual melanoma subtype results, see **Table 4** and for a visualization of the differences, see **Supplementary Fig. 3**). Thereby, a total of 623 of 653 melanomas (0.954 sensitivity) were detected by either the AI, the dermatologist or both. Concurrently, ADAE classified 618 of 918 non-melanoma correctly (0.673 specificity), while dermatologists classified 760 of 918 non-melanoma (0.828 specificity) correctly. A total of 833 of 918 non-melanoma (0.907 specificity) were classified correctly by either the AI, the dermatologist or both. Thus, the combination could exceed the individual outcomes of both AI and dermatologist, wherein solitary ADAE exhibited a higher detection, but also a higher false positive rate than dermatologists. Hence, a synergistic approach could benefit patients more than relying on man or machine alone.

Subset analyses

Additionally, multiple subset analyses were performed to identify disparities in diagnostic performance, revealing substantial differences within certain subsets.

Melanoma subtypes

The algorithm showed significantly higher sensitivity on all melanoma subtypes except for nodular melanoma than dermatologists ($p < 0.001$ for all comparisons, see **Table 4**).

Data source

Moreover, the algorithm achieved a better balanced accuracy than dermatologists on data derived from five out of seven hospitals (i.e. the data of the test set, excluding the validation data from hospital 8, see **Table 3**), but performed significantly worse on data from hospital 1 (0.772, 95% CI 0.742-0.803 vs. 0.783, 95% CI 0.751-0.817; $p < 0.001$), and hospital 3 (0.615, 95% CI 0.521-0.716 vs. 0.758, 95% CI 0.659-0.860; $p < 0.001$). The dermatologists' sensitivity was worse for all data except those from hospital 3 (0.897, 95% CI 0.806-0.976 vs. 0.923, 95% CI 0.823-1.000; $p < 0.001$), while their specificity was higher without exception. Although consistent with the overall test set results, this observation highlights hospital 3 as an outlier.

Patient age and lesion location

Furthermore, ADAE achieved significantly higher balanced accuracy in patients younger than 35 years (0.890, 95% CI 0.859-0.920 vs. 0.767, 95% CI 0.636-0.897; $p < 0.001$), and for lesions on the head or neck (0.775, 95% CI 0.726-0.822 vs. 0.660, 95% CI 0.603-0.714; $p < 0.001$) but performed significantly worse for lesions on the palms or soles (0.649, 95% CI 0.508-0.774 vs. 0.798, 95% CI 0.642-0.944; $p < 0.001$) compared to dermatologists.

Classification complexity

The dermatologists indicated the level of confidence they had in their own diagnosis on a scale from 1 (low confidence) to 5 (high confidence), signifying the perceived classification

complexity of the lesion. Based on these data, the algorithm demonstrated significantly higher balanced accuracy than the dermatologists on lesions that were assigned lower confidence scores (confidence score 1: 0.754, 95% CI 0.608-0.895 vs. 0.508, 95% CI 0.357-0.688; confidence score 2: 0.761, 95% CI 0.689-0.829 vs. 0.588, 95% CI 0.491-0.680; confidence score 3: 0.767, 95% CI 0.729-0.804 vs. 0.662, 95% CI 0.615-0.709; confidence score 4: 0.811, 95% CI 0.782-0.839 vs. 0.805, 95% CI 0.775-0.838; $p < 0.001$ for all comparisons) but lower balanced accuracy for lesions diagnosed with a confidence score of 5 (0.820, 95% CI 0.779-0.858 vs. 0.899, 95% CI 0.871-0.925; $p < 0.001$). Hence, the AI algorithm seems less susceptible to the diagnostic difficulty. This also indicates that dermatologists assess their own prediction somewhat accurately, and especially when unsure could benefit greatly from such an AI prediction.

ADAE generalizes robustly on different subsets

The predictive quality of AI algorithms may depend on certain features of the test set, such as data source, patient age, lesion size or location. To analyze whether the algorithm in this study demonstrates robust generalizability, we evaluated the association between the predictions and specific stratified domains included in the heterogeneous dataset used for classifier testing (see **Table 3** for test set characteristics). Therefore, the Breslow-Day test for homogeneity of the odds ratio was used. For inter-AI comparisons, the area under the receiver operating characteristic curve (AUROC) in combination with DeLong's method is used as a more objective alternative than accuracy, since it is independent of a threshold setting. P-values smaller than 0.05 are considered statistically significant.

ADAE prediction generalizability

Overall, there was no significant association between the ADAE prediction and the patient age ($p=0.104$), skin type ($p=0.587$; excluding unknown skin types, and skin types V+VI due to a low sample size (<25)), or lesion location domain ($p=0.233$; excluding lesions in unknown locations, and oral/genital lesions due to a low sample size (<25)), the technical domain (i.e.,

camera setup; $p=0.068$) or the dermatologists' diagnostic confidence score, although borderline significant ($p=0.050$). However, a significant association with lesion diameter ($p=0.009$) and data source (i.e., the originating hospital; $p=0.027$) was identified, indicating that performance correlates with these features. Specifically, the algorithm performed significantly worse on data from hospital 3, as indicated by the lower AUROC score (hospital 3: 0.775, 95% CI 0.660-0.877 vs. other hospitals combined: 0.921, 95% CI 0.906-0.934; $p=0.013$). Without the outlier dataset (hospital 3), there was no significant association between the predictive performance and data source ($p=0.416$). Furthermore, the AUROC was significantly higher for lesions with diameters greater than 6 mm (≤ 6 mm: 0.802, 95% CI, 0.747-0.857 vs. > 6 mm: 0.917, 95% CI, 0.901-0.932; $p<0.001$). These findings suggest that the algorithm has robust generalization capabilities on most domains, while it is influenced by lesion diameter and data source.

While not all differences exhibited by ADAE within each subset were significant, the disparities between upper and lower bound within some subsets were significant. Specifically, for patient age, ADAE achieved a higher AUROC score for the youngest patients than for the oldest ones (<35 : 0.974, 95% CI 0.942-0.997 vs. >74 : 0.879, 95% CI 0.847-0.909; $p<0.001$). Similarly, for the Fitzpatrick skin type, the lightest skin type was associated with lower AUROCs than the darkest one (type I: 0.865, 95% 0.802-0.922 vs. type IV: 0.985, 95% CI 0.943-1.000; $p<0.001$). Thus, even though the algorithm generalizes robustly, certain trends are still evident, signifying partial dependencies with respect to some groups of lesions or patients, which can still affect diagnostic performance.

Dermatologist prediction generalizability

Among dermatologists, on the other hand, there were no significant associations between prediction and skin type (excluding unknown skin types and V+VI due to low sample size (<25); $p=0.750$), lesion diameter ($p=0.164$), technical domain ($p=0.862$), or data source ($p=0.527$). There were, however, significant associations of the prediction with patient age

($p < 0.001$), lesion location (excluding unknown locations, and oral/genital locations due to low sample size (< 25); $p < 0.001$), and the dermatologist diagnostic confidence ($p < 0.001$). These findings indicate that the prediction quality of the dermatologists depends on these features. Specifically, the dermatologists' specificity decreased with increasing patient age (< 35 years: 0.963, 95% CI 0.932-0.988 vs. 35-54 years: 0.863, 95% CI 0.819-0.902; vs. 55-74 years: 0.813, 95% CI 0.766-0.859; vs. > 74 years: 0.697, 95% CI 0.632-0.757; $p < 0.001$ for all comparisons). Relatedly, sensitivity was significantly lower for patients younger than 35 years (< 35 years: 0.571, 95% CI 0.308-0.833 vs. all other age groups combined: 0.737, 95% CI 0.703-0.771; $p < 0.001$) but followed similar trends as the specificity for age groups older than 35 years (35-54 years: 0.780, 95% CI 0.692-0.850 vs. 55-74 years: 0.739, 95% CI 0.688-0.788; vs. > 74 years: 0.716, 95% CI 0.659-0.773; $p < 0.001$ for all comparisons). Additionally, the dermatologists' balanced accuracy was significantly lower for lesions on the head or neck (head/neck: 0.660, 95% CI 0.603-0.714 vs. all other locations combined: 0.810, 95% CI 0.788-0.832; $p < 0.001$) but was higher for lesions that received higher dermatologists' confidence scores (confidence score 1: 0.508, 95% CI 0.357-0.688 vs. confidence score 2: 0.588, 95% CI 0.491-0.680; vs. confidence score 3: 0.662, 95% CI 0.615-0.709; vs. confidence score 4: 0.806, 95% CI 0.775-0.838; vs. confidence score 5: 0.899, 95% CI 0.871-0.925; $p < 0.001$ for all comparisons).

Discussion

In this multicenter study with prospectively collected samples, we evaluated the diagnostic performance of ADAE in differentiating between melanoma and non-melanoma skin lesions and compared it to dermatologists' diagnostic accuracy as recorded during real-life patient examinations. One of the main strengths of the study in addition to the prospective data collection is its comprehensive test set, which includes a wide range of melanoma subtypes and lesion locations encountered in routine care. Altogether, ADAE performed better than dermatologists in terms of balanced accuracy and sensitivity, but achieved a lower specificity. Moreover, the algorithm generalized robustly to domains such as patient age and skin type, lesion location, and camera setup, but its performance was affected by lesion diameter. The dermatologists' diagnostic accuracy, in contrast, correlated significantly with patient age and lesion location.

To evaluate AI algorithms for melanoma detection, we measured the performance of ADAE against dermatologists using a prospectively collected, heterogeneous dataset. ADAE performed better in terms of balanced accuracy (ADAE: 0.798 vs. dermatologists: 0.781), and achieved a higher sensitivity (0.922 vs. 0.734) at the cost of a lower specificity (0.673 vs. 0.828). Additionally, our findings suggest that AI algorithms may be better suited than dermatologists for diagnosing skin lesions of younger patients or patients with lesions on the head or neck, as indicated by the balanced accuracy in these tasks (<35 years: 0.890 vs. 0.767 and head/neck: 0.775 vs. 0.660, respectively). In contrast, dermatologists were significantly better at diagnosing lesions on acral skin, i.e. on the palms or soles (0.649 vs. 0.798). Interestingly, in our study, the algorithm exhibited significantly higher diagnostic accuracy in cases where dermatologists tended to be unsure, thus highlighting the potential synergies between AI and human experts. Our findings are in line with previous studies^{7,10,11,13,19-21} that demonstrated the potential advantages arising from the cooperation of dermatologists with AI. Our study addresses the limitations of previous studies, specifically by

our multicenter design encompassing a substantial number of dermatologists, a larger cohort of lesions and rare melanoma subtypes. *Marchetti et al*¹³ previously analyzed ADAE in terms of classification performance and its impact on dermatologists' decisions, but are limited by a small test set. We compare our results to underscore their external validity. Our overall AUROC was slightly higher than *Marchetti et al* reported (without R-TTA: 0.898, 95% CI 0.884-0.913 vs. 0.858). The subset analyses were also largely similar between the studies: the performance of ADAE was worse for older patients, and those with type I skin in both studies. Specificity was lower for the larger lesions, despite the increase in AUROC. However, unlike in our study, *Marchetti et al* reported a lower specificity of the algorithm for head/neck area lesions. These findings suggest that a collaborative^{13,19} rather than a comparative approach^{7,10,11,20} may ultimately lead to an improvement in patient care, achieving an increased detection rate while reducing the number of unnecessary excisions as compared to relying solely on either dermatologists or AI alone.

When we investigated the effect of the different variables on diagnostic performance, we found differences in those effects between the AI algorithm and dermatologists. Specifically, the performance of the AI was affected by the lesion diameter; it performed worse for lesions with diameters smaller than 6 mm while dermatologists discriminated lesions of all sizes relatively consistently. Concurrently, the dermatologists' decisions but not those of ADAE were influenced by patient age and lesion location. This further underscores the advantages of a holistic approach, as the diagnostic strengths of the AI and dermatologists may compensate for each other's shortcomings in their generalization abilities.

While the algorithm was largely unaffected by the data source (i.e., the hospital), it performed significantly worse on data from one particular hospital, hospital 3. The population of this hospital comprised older individuals when compared to the other hospitals (age at diagnosis: hospital 3: 27 to 96, median of 65.5 years vs. other hospitals: 18 to 95, median of 63 years) while exhibiting a slightly different distribution of skin types from the overall study population

(i.e., a preponderance of type I and II skin types). Although we did find that ADAE performed worse for older patients and those with lighter skin types, this finding requires further investigation to identify potential confounders.

While our study comprises multiple centers, they are all located in Germany. Thus, our findings might not translate to other ethnicities or skin types (especially types V and VI, which are underrepresented in our study). Furthermore, we are limited to a binary classification (melanoma vs. non-melanoma), which does not fully model the complexity of clinical reality, which involves lesion classification into multiple classes. Finally, our comparison of AI and dermatologists was performed by comparing diagnostic accuracy and generalization, but does not include other metrics and aspects, such as the for ensembles typically problematic computing costs and explainability, nor does it investigate a prospective impact on dermatologists' management decisions. Especially explainability is a feature of AI that is both required by EU standards for transparency in AI^{22,23} and demanded by physicians and patients alike.²⁴⁻²⁷ In a recent retrospective study, a dermatologist-like explainable AI enhanced trust and confidence in diagnosing melanoma among 116 participating clinicians, promoting its future use in care.²¹ Future research could build upon this work by evaluating different AI architectures, such as model soups^{28,29}, that use the average weights of multiple models to improve performance, and addresses the ensemble drawbacks, namely performance costs as well as explainability aspects.

In conclusion, ADAE showed better performance than dermatologists in terms of balanced accuracy and sensitivity, but worse specificity. It generalizes robustly on most domains of a heterogenous, prospectively collected test set. Thus, it could be particularly useful in medical settings, where there often is a large discrepancy between hospitals due to technical differences related to imaging and sometimes patient populations. Ultimately, AI algorithms can support physicians in their diagnoses to identify melanomas more accurately, especially for difficult cases in which the human dermatologists are unsure of their diagnoses. Future

research should address the shortcomings of the algorithm, such as lack of explainability and the low specificity, both particularly problematic to facilitate the clinical use of AI.

Methods

Study Design

This prospective, multicenter study was approved by the respective institutional review boards of the participating centers and adheres to the Declaration of Helsinki guidelines. The STARD 2015 reporting standards³⁰ (see **Supplementary Table 2**) were followed, and written informed consent was obtained from all participating patients.

Data on clinically suspected melanomas that were subsequently excised, consisting of dermoscopic images and patient-specific metadata (including age, Fitzpatrick skin type, lesion localization, and diameter), were prospectively gathered as part of routine clinical practice from eight university hospitals in Germany (located in Berlin, Dresden, Erlangen, Essen, Mannheim, Munich, Regensburg, and Wuerzburg) between April 2021 and March 2023.

Participants

Participants for this study were eligible if they met all of the following criteria: at least 18 years of age and presenting with clinically melanoma-suspicious skin lesions. Patients were excluded if these melanoma-suspicious lesions had undergone pre-biopsy procedures, were located near the eye or beneath the fingernails or toenails, or had person-identifying features (such as tattoos) in the immediate vicinity of the lesion due to data privacy concerns.

Data collection

After informed consent, imaging and dermoscopic examination were performed and melanoma-suspicious lesions were subsequently excised. All lesions were histopathologically diagnosed by at least one experienced (dermato)pathologist at the respective hospital. During clinical examinations, a dermatologist captured six dermoscopic images of each suspected melanoma lesion while deliberately introducing random variations in the orientation/angle, position, and operational mode of the dermatoscope, including both polarized and

nonpolarized settings. Dermatologist hereby is defined as a doctor who studies and treats skin diseases in a Department of Dermatology, but has not necessarily completed board-certification yet. To mitigate the influence of potential confounding variables, dermatologists were explicitly instructed to avoid known artifacts (such as skin markings). All images were acquired using one of four distinct hardware configurations that were consistently used across the participating medical centers (see **Supplementary Methods**).

Model Training and Testing

As we employed the ready-to-use ADAE algorithm for binary classification of lesion images into melanoma and non-melanoma, no additional training was needed. ADAE is trained solely on public data from the respective 2020 and 2019 (which includes 2018 data) SIIM-ISIC challenges, comprising a total of 58,457 lesions, 5106 of which were labeled melanoma.^{31–34} The ensemble consists of 18 convolutional neural network (CNN)-models (16 EfficientNets B3-7, 1 SE-ResNext101, 1 ResNest101), of which four additionally incorporate patient meta-data (including sex, age, and lesion location). Since the best model of each 5-fold cross-validation is kept, this totals to 90 models in the final ensemble (for a detailed description of the algorithm and its training procedure, please refer to the original paper¹⁶).

To ensure that the algorithm runs correctly, it was tested on the SIIM-ISIC 2020 data according to a publicly available script on GitHub (<https://github.com/ISIC-Research/ADAE/predict.py>). The resulting AUROC scores match those available in the literature (ISIC validation: ours 0.945 vs. literature 0.949, ISIC test: 0.951 vs. 0.950).^{13,17}

Since our dataset includes six images per lesion, ADAE is adapted with R-TTA to utilize these additional images, as this has proven to be beneficial with respect to diagnostic performance, robustness and uncertainty estimation.¹⁸ There, all six real images are fed to the algorithm at test time, and the resulting outputs are then aggregated to one final prediction. A comparison of the diagnostic accuracy of ADAE with versus without R-TTA is shown in **Supplementary**

Figs. 6 and 7, which also include the scores for the individual models that the ensemble comprises.

To find a suitable threshold differentiating positive from negative predictions, a validation set was split from the data, namely, the data of hospital 8, as it also has its own unique technical domain while being sufficiently large enough to allow for a representative estimate. Therefore, the threshold is set such that a sensitivity of at least 85% is exceeded, as sensitivities of approximately 80-85% are realistic in a clinical setting.^{9,35,36}

Statistical Analysis

The difference between ADAE and dermatologists' diagnostic accuracy was primarily quantified through balanced accuracy, and secondarily via sensitivity and specificity. For each endpoint, pairwise two-sided Wilcoxon signed-rank tests were used to compare the respective metrics. To evaluate the generalizability of the algorithm on different subsets, the Breslow-Day test for homogeneity of the odds ratio was used.³⁷ Hypothesis H0 is a constant odds ratio over a stratified variable k , indicating whether there is a significant association between prediction and k . The algorithm's predictive ability was assessed using the AUROC. Differences in model performance were assessed by statistically comparing the corresponding AUROCs using DeLong's method.³⁸

To reduce the impact of stochastic events, mean values for each metric were calculated using 1000 bootstrap iterations. The corresponding 95% confidence intervals (CIs) were determined using the nonparametric percentile method. P-values smaller than 0.05 were considered statistically significant. Statistical analysis was performed using SciPy 1.11.2³⁹ and R⁴⁰.

Data availability

The pretrained ADAE algorithm is publicly available via GitHub <https://github.com/ISIC-Research/ADAE>. The SIIM-ISIC 2020 data is publicly available at <https://challenge2020.isic-archive.com/>. Our dataset is available from the corresponding author on reasonable request.

Abbreviations

AI	artificial intelligence
ADAE	All Data Are Ext
SIIM	Society for Imaging Informatics in Medicine
ISIC	International Skin Image Collaboration
R-TTA	real test-time augmentation
CI	confidence interval
AUROC	area under the receiver operating characteristic curve
CNN	convolutional neural network

References

1. Guy, G. P., Jr *et al.* Vital signs: melanoma incidence and mortality trends and projections - United States, 1982-2030. *MMWR Morb. Mortal. Wkly. Rep.* **64**, 591–596 (2015).
2. Matthews, N. H., Li, W.-Q., Qureshi, A. A., Weinstock, M. A. & Cho, E. Epidemiology of Melanoma. *Exon Publications* 3–22 (2017).
3. Lens, M. B. & Dawes, M. Global perspectives of contemporary epidemiological trends of cutaneous malignant melanoma. *Br. J. Dermatol.* **150**, 179–185 (2004).
4. Petrie, T., Samatham, R., Witkowski, A. M., Esteva, A. & Leachman, S. A. Melanoma Early Detection: Big Data, Bigger Picture. *J. Invest. Dermatol.* **139**, 25–30 (2019).
5. Rigel, D. S., Russak, J. & Friedman, R. The evolution of melanoma diagnosis: 25 years beyond the ABCDs. *CA Cancer J. Clin.* **60**, 301–316 (2010).
6. Carli, P. *et al.* The problem of false-positive diagnosis in melanoma screening: the impact of dermoscopy. *Melanoma Res.* **13**, 179–182 (2003).
7. Haenssle, H. A. *et al.* Man against machine: diagnostic performance of a deep learning convolutional neural network for dermoscopic melanoma recognition in comparison to 58 dermatologists. *Ann. Oncol.* **29**, 1836–1842 (2018).
8. Watson, A. J. & Kvedar, J. C. Staying on top in dermatology: why we must act now to address the capacity challenge. *Arch. Dermatol.* **144**, 541–544 (2008).
9. Hagggenmüller, S. *et al.* Skin cancer classification via convolutional neural networks: systematic review of studies involving human experts. *Eur. J. Cancer* **156**, 202–216 (2021).
10. Esteva, A. *et al.* Dermatologist-level classification of skin cancer with deep neural networks. *Nature* **542**, 115–118 (2017).
11. Tschandl, P. *et al.* Expert-Level Diagnosis of Nonpigmented Skin Cancer by Combined Convolutional Neural Networks. *JAMA Dermatol.* **155**, 58–65 (2019).
12. Brancaccio, G. *et al.* Artificial Intelligence in Skin Cancer Diagnosis: A Reality Check. *J.*

- Invest. Dermatol.* (2023) doi:10.1016/j.jid.2023.10.004.
13. Marchetti, M. A. *et al.* Prospective validation of dermoscopy-based open-source artificial intelligence for melanoma diagnosis (PROVE-AI study). *npj Digital Medicine* **6**, 1–11 (2023).
 14. Phillips, M. *et al.* Assessment of Accuracy of an Artificial Intelligence Algorithm to Detect Melanoma in Images of Skin Lesions. *JAMA Netw Open* **2**, e1913436 (2019).
 15. The use of noninvasive imaging techniques in the diagnosis of melanoma: a prospective diagnostic accuracy study. *J. Am. Acad. Dermatol.* **85**, 353–359 (2021).
 16. Ha, Q., Liu, B. & Liu, F. Identifying Melanoma Images using EfficientNet Ensemble: Winning Solution to the SIIM-ISIC Melanoma Classification Challenge. (2020).
 17. SIIM-ISIC Melanoma Classification. <https://kaggle.com/competitions/siim-isic-melanoma-classification>.
 18. Hekler, A. *et al.* Using Multiple Dermoscopic Photographs of One Lesion Improves Melanoma Classification via Deep Learning: A Prognostic Diagnostic Accuracy Study. (2023).
 19. Winkler, J. K. *et al.* Assessment of Diagnostic Performance of Dermatologists Cooperating With a Convolutional Neural Network in a Prospective Clinical Study: Human With Machine. *JAMA Dermatol.* **159**, 621–627 (2023).
 20. Superior skin cancer classification by the combination of human and artificial intelligence. *Eur. J. Cancer* **120**, 114–121 (2019).
 21. Chanda, T. *et al.* Dermatologist-like explainable AI enhances trust and confidence in diagnosing melanoma. *Nat. Commun.* **15**, 524 (2024).
 22. Explainable artificial intelligence in skin cancer recognition: A systematic review. *Eur. J. Cancer* **167**, 54–69 (2022).
 23. *White Paper on Artificial Intelligence: A European Approach to Excellence and Trust.* (2020).
 24. Jutzi, T. B. *et al.* Artificial Intelligence in Skin Cancer Diagnostics: The Patients' Perspective. *Front. Med.* **7**, 233 (2020).

25. Nelson, C. A. *et al.* Patient Perspectives on the Use of Artificial Intelligence for Skin Cancer Screening: A Qualitative Study. *JAMA Dermatol.* **156**, 501–512 (2020).
26. The role of explainability in creating trustworthy artificial intelligence for health care: A comprehensive survey of the terminology, design choices, and evaluation strategies. *J. Biomed. Inform.* **113**, 103655 (2021).
27. Amann, J., Blasimme, A., Vayena, E., Frey, D. & Madai, V. I. Explainability for artificial intelligence in healthcare: a multidisciplinary perspective. *BMC Med. Inform. Decis. Mak.* **20**, 1–9 (2020).
28. Model soups improve performance of dermoscopic skin cancer classifiers. *Eur. J. Cancer* **173**, 307–316 (2022).
29. Wortsman, M. *et al.* Model soups: averaging weights of multiple fine-tuned models improves accuracy without increasing inference time. in *International Conference on Machine Learning* 23965–23998 (PMLR, 2022).
30. Bossuyt, P. M. *et al.* STARD 2015: an updated list of essential items for reporting diagnostic accuracy studies. *BMJ* **351**, h5527 (2015).
31. The. *ISIC 2020 Challenge Dataset* <https://doi.org/10.34970/2020-ds01>.
32. Tschandl, P., Rosendahl, C. & Kittler, H. The HAM10000 dataset, a large collection of multi-source dermoscopic images of common pigmented skin lesions. *Scientific Data* **5**, 1–9 (2018).
33. Codella, N. C. F. *et al.* Skin Lesion Analysis Toward Melanoma Detection: A Challenge at the 2017 International Symposium on Biomedical Imaging (ISBI), Hosted by the International Skin Imaging Collaboration (ISIC). (2017).
34. Combalia, M. *et al.* BCN20000: Dermoscopic Lesions in the Wild. (2019).
35. Vestergaard, M. E., Macaskill, P., Holt, P. E. & Menzies, S. W. Dermoscopy compared with naked eye examination for the diagnosis of primary melanoma: a meta-analysis of studies performed in a clinical setting. *Br. J. Dermatol.* **159**, 669–676 (2008).
36. Phillips, M., Greenhalgh, J., Marsden, H. & Palamaras, I. Detection of Malignant Melanoma Using Artificial Intelligence: An Observational Study of Diagnostic Accuracy.

Dermatol Pract Concept e2020011–e2020011 (2019).

37. Breslow, N. E. & Day, N. E. Statistical methods in cancer research. Volume I - The analysis of case-control studies. *IARC Sci. Publ.* 5–338 (1980).
38. DeLong, E. R., DeLong, D. M. & Clarke-Pearson, D. L. Comparing the areas under two or more correlated receiver operating characteristic curves: a nonparametric approach. *Biometrics* **44**, 837–845 (1988).
39. Virtanen, P. *et al.* SciPy 1.0: fundamental algorithms for scientific computing in Python. *Nat. Methods* **17**, 261–272 (2020).
40. The R Project for Statistical Computing. <https://www.R-project.org/>.

Author Contributions

Dr Brinker had full access to all the data in the study and takes responsibility for the integrity of the data and the accuracy of the data analysis.

Concept and design: Hekler, Maron, Brinker, Heinlein, Haggenmüller.

Acquisition, analysis, or interpretation of data: All authors.

Drafting of the manuscript: Hekler, Maron, Heinlein.

Critical revision of the manuscript for important intellectual content: All authors.

Statistical analysis: Hekler, Maron, Heinlein, Haggenmüller, Wies.

Obtained funding: Brinker.

Administrative, technical, or material support: Hekler, Maron, Haggenmüller, Brinker.

Supervision: Hekler, Haggenmüller, Brinker.

Conflict of Interest Disclosures

Jochen S. Utikal is on the advisory board or has received honoraria and travel support from Amgen, Bristol Myers Squibb, GSK, Immunocore, LeoPharma, Merck Sharp and Dohme, Novartis, Pierre Fabre, Roche and Sanofi outside the submitted work. **Friedegund Meier** has received travel support and/or speaker's fees and/or advisor's honoraria by Novartis, Roche, BMS, MSD and Pierre Fabre and research funding from Novartis and Roche. **Sarah Hobelsberger** reports clinical trial support from Almirall and speaker's honoraria from Almirall, UCB and AbbVie and has received travel support from the following companies: UCB, Janssen Cilag, Almirall, Novartis, Lilly, LEO Pharma and AbbVie outside the submitted work. **Sebastian Haferkamp** reports advisory roles for or has received honoraria from Pierre Fabre Pharmaceuticals, Novartis, Roche, BMS, Amgen and MSD outside the submitted work. **Konstantin Drexler** has received honoraria from Pierre Fabre Pharmaceuticals and Novartis. **Axel Hauschild** reports clinical trial support, speaker's honoraria, or consultancy fees from the following companies: Agenus, Amgen, BMS, Dermagnostix, Highlight Therapeutics, Immunocore, Incyte, IO Biotech, MerckPfizer, MSD, NercaCare, Novartis, Philogen, Pierre

Fabre, Regeneron, Roche, Sanofi-Genzyme, Seagen, Sun Pharma and Xenthera outside the submitted work. **Lars E. French** is on the advisory board or has received consulting/speaker honoraria from Galderma, Janssen, Leo Pharma, Eli Lilly, Almirall, Union Therapeutics, Regeneron, Novartis, Amgen, AbbVie, UCB, Biotest and InflaRx. **Max Schlaak** reports advisory roles for Bristol-Myers Squibb, Novartis, MSD, Roche, Pierre Fabre, Kyowa Kirin, Immunocore and Sanofi-Genzyme. **Wiebke Sondermann** reports grants, speaker's honoraria, or consultancy fees from medi GmbH Bayreuth, AbbVie, Almirall, Amgen, Bristol-Myers Squibb, Celgene, GSK, Janssen, LEO Pharma, Lilly, MSD, Novartis, Pfizer, Roche, Sanofi Genzyme and UCB outside the submitted work. **Bastian Schilling** reports advisory roles for or has received honoraria from Sanofi, Pierre Fabre Pharmaceuticals, SUN Pharma and BMS, research funding from Novartis, all outside the submitted work. **Matthias Goebeler** has received speaker's honoraria and/or has served as a consultant and/or member of advisory boards for Almirall, Argenx, Biotest, Eli Lilly, Janssen Cilag, Leo Pharma, Novartis and UCB outside the submitted work. **Michael Erdmann** declares honoraria and travel support from Bristol-Myers Squibb, Immunocore Novartis, Pierre Farbe, and Sanofi outside the submitted work. **Jakob N. Kather** reports consulting services for Owkin, France, Panakeia, UK and DoMore Diagnostics, Norway and has received honoraria for lectures by MSD, Eisai and Fresenius. **Titus J. Brinker** reports owning a company that develops mobile apps (Smart Health Heidelberg GmbH, Handschuhsheimer Landstr. 9/1, 69120 Heidelberg). The remaining authors declare that the research was conducted in the absence of any commercial or financial relationships that could be construed as a potential conflict of interest.

Funding/Support

This study was funded by the Federal Ministry of Health, Berlin, Germany (grant: Skin Classification Project 2; grant holder: Titus J. Brinker, German Cancer Research Center, Heidelberg, Germany).

Role of the Funder/Sponsor

The sponsor had no role in the design and conduct of the study; collection, management, analysis and interpretation of the data; preparation, review, or approval of the manuscript; and decision to submit the manuscript for publication.

Tables

Table 1. Patient characteristics of our dataset

Patient characteristic	N = 1716	%
Age [mean (std, IQR)]	60.9	(18.3, 28)
Sex		
Male	985	57.4
Female	731	42.6
Fitzpatrick skin type		
I	138	8.04
II	1011	58.9
III	477	27.8
IV	37	2.16
V	3	0.175
VI	3	0.175
unknown	47	2.74
Personal history of melanoma		
No	1320	76.9
Yes	335	19.5
Unknown	61	3.55
Family history of melanoma		
No	1495	87.1
Yes	123	7.17
Unknown	98	5.71
Number of enrolled lesions		
1	1522	88.7
2	194	11.3

Table 2. Lesion characteristics of our dataset. The different technical setups (technical domain) are explained in detail in the **Supplementary Methods**.

Lesion characteristic	N = 1910	%
Type		
Melanoma	750	39.3
Nevus	885	46.3
Other	275	14.4
Melanoma subtypes	(N=750)	
Superficial spreading	339	45.2
Other	219	29.2
Nodular	64	8.53
Lentigo maligna	64	8.53
Acral lentiginous	24	3.20
Combined forms of melanoma	19	2.53

Unknown	12	1.60
Nevoid	3	0.40
Desmoplastic	3	0.40
Spitzoid	3	0.40
Location (grouped)		
Posterior torso	576	30.2
Lower extremity	361	18.9
Anterior torso	344	18.0
Head/neck	333	17.4
Upper extremity	236	12.4
Palms/soles	35	1.83
Oral/genital	19	0.995
Unknown	6	0.314
Diameter (in mm)		
<=3.00	180	9.42
3.01-6.00	481	25.2
6.01-9.00	290	15.2
9.01-12.00	378	19.8
12.01-15.00	195	10.2
>15.00	386	20.2
Hospital		
Hospital 1	567	29.7
Hospital 2	265	13.9
Hospital 3	66	3.46
Hospital 4	215	11.3
Hospital 5	106	5.55
Hospital 6	176	9.21
Hospital 7	176	9.21
Hospital 8	339	17.7
Pigmented lesion		
Yes	1817	95.1
No	51	2.67
Unknown	42	2.20
Technical domain		
Setup 1	898	47.0
Setup 2	321	16.8
Setup 3	352	18.4
Setup 4	339	17.7
Dermatologists' confidence rating		
1	36	1.88
2	119	6.23
3	748	39.2
4	578	30.3
5	429	22.5

Table 3: Diagnostic performance of dermatologists and ADAE for various subsets of our test set (i.e., validation samples are not included here). Bal. acc.: Balanced accuracy, Sens.: Sensitivity, Spec.: Specificity, AUROC: Area under the receiver operating characteristic curve

Characteristic	Total lesions (n)	Total melanomas (n)	Dermatologists			ADAE			
			Bal. acc.	Sens.	Spec.	AUR OC	Bal. acc.	Sens.	Spec.
Overall	1571	653	0.781	0.734	0.828	0.916	0.798	0.922	0.673
Age (in years)									
<35	177	14	0.767	0.571	0.963	0.974	0.890	1.000	0.779
35-54	372	109	0.821	0.780	0.863	0.931	0.818	0.945	0.692
55-74	571	287	0.776	0.739	0.813	0.913	0.793	0.913	0.673
>74	451	243	0.707	0.716	0.697	0.879	0.743	0.918	0.567
Sex									
Male	896	399	0.760	0.734	0.785	0.909	0.783	0.920	0.646
Female	675	254	0.806	0.732	0.879	0.923	0.815	0.925	0.705
Hospital									
Hospital 1	567	245	0.783	0.669	0.898	0.901	0.772	0.914	0.630
Hospital 2	265	123	0.764	0.709	0.819	0.922	0.810	0.891	0.729
Hospital 3	66	39	0.758	0.923	0.593	0.775	0.615	0.897	0.333
Hospital 4	215	93	0.765	0.748	0.783	0.937	0.828	0.959	0.696
Hospital 5	106	31	0.800	0.774	0.827	0.932	0.852	0.903	0.800
Hospital 6	176	67	0.739	0.716	0.761	0.890	0.771	0.881	0.661
Hospital 7	176	55	0.806	0.817	0.795	0.934	0.822	0.957	0.687
Location (grouped)									
Posterior torso	469	196	0.791	0.765	0.817	0.920	0.788	0.923	0.652
Anterior torso	294	80	0.804	0.725	0.883	0.951	0.833	0.938	0.729
Lower extremity	293	116	0.856	0.853	0.859	0.935	0.817	0.957	0.678
Head/neck	278	137	0.660	0.562	0.759	0.881	0.775	0.883	0.667
Upper extremity	191	111	0.778	0.757	0.800	0.893	0.784	0.919	0.650
Palms/soles	29	11	0.798	0.818	0.778	0.798	0.649	0.909	0.389
Oral/genital	12	1	0.864	1.000	0.727	0.818	0.818	1.000	0.636
Unknown	5	1	0.875	1.000	0.750	1.000	1.000	1.000	1.000
Diameter (in mm)									
<=3.00	120	14	0.784	0.643	0.925	0.806	0.772	0.714	0.830
3.01-6.00	387	62	0.660	0.419	0.902	0.797	0.715	0.726	0.705
6.01-9.00	274	89	0.695	0.584	0.805	0.895	0.796	0.921	0.670
9.01-12.00	313	155	0.782	0.735	0.829	0.924	0.803	0.929	0.677
12.01-15.00	151	94	0.713	0.777	0.649	0.918	0.765	0.968	0.561
>15.00	326	239	0.728	0.858	0.598	0.890	0.700	0.962	0.437
Fitzpatrick skin type									
I	149	77	0.797	0.857	0.736	0.865	0.760	0.922	0.597
II	797	390	0.778	0.708	0.848	0.912	0.796	0.918	0.673
III	531	160	0.774	0.731	0.817	0.938	0.821	0.931	0.712
IV	39	9	0.839	0.778	0.900	0.985	0.783	1.000	0.567
V	3	1	1.000	1.000	1.000	1.000	0.750	1.000	0.500
VI	2	0	0.500	-	0.500	-	0.000	-	0.000
Unknown	50	16	0.801	0.750	0.853	0.877	0.717	0.875	0.559
Technical domain									
Setup 1	898	339	0.779	0.705	0.853	0.903	0.781	0.909	0.653
Setup 2	321	154	0.778	0.753	0.802	0.943	0.845	0.948	0.743

Setup 3	352	160	0.776	0.775	0.776	0.912	0.798	0.925	0.672
Dermatologists' confidence rating									
1	36	13	0.508	0.538	0.478	0.913	0.754	0.769	0.739
2	111	34	0.588	0.500	0.675	0.851	0.761	0.912	0.610
3	424	141	0.662	0.546	0.777	0.860	0.767	0.872	0.661
4	575	206	0.806	0.733	0.878	0.934	0.811	0.942	0.680
5	425	259	0.899	0.876	0.922	0.939	0.820	0.942	0.699

Table 4. Detection rate for each melanoma subtype.

Melanoma subtype	Dermatologist			ADAE			Total n	p-Value
	n	Sens.	95% CI	n	Sens.	95% CI		
Superficial spreading	228	0.820	0.773-0.863	266	0.957	0.932-0.978	278	p<0.001
Other	127	0.583	-	192	0.881	-	218	-
Nodular	56	0.982	0.947-1.000	55	0.965	0.912-1.000	57	p<0.001
Lentigo maligna	27	0.600	0.466-0.733	41	0.911	0.822-0.978	45	p<0.001
Acral lentiginous	16	0.842	0.684-1.000	17	0.895	0.737-1.000	19	p<0.001
Combined forms of melanoma	12	0.667	0.444-0.889	17	0.944	0.833-1.000	18	p<0.001
Unknown	6	0.667	-	7	0.778	-	9	-
Nevoid	3	1.000	-	3	1.000	-	3	-
Desmoplastic	2	0.667	-	1	0.333	-	3	-
Spitzoid	2	0.667	-	3	1.000	-	3	-
Total	479	73.35		602	92.19		653	

Supplementary Materials

Supplementary Methods

Dataset description

The four hardware settings across the clinics were as follows:

- Setup1: HEINE IC1 dermatoscope with an Apple iPhone7
- Setup2: HEINE DELTAone dermatoscope with an Apple iPhone SE
- Setup3: HEINE Delta30 dermatoscope with an Apple iPhone 7
- Setup4: HEINE DELTAone dermatoscope with an Apple iPhone8

The original images were automatically cropped to exclude large parts of the black image margin which originates from dermoscopy and subsequently resized to 512x512, 768x768, and 1024x1024 pixels respectively for model inference.

Since the original location annotations are more fine-grained than the required input for the models requiring metadata, the following mapping is used (location grouped: location1, location2, ...):

- anterior torso: abdomen, chest
- head/neck: face, scalp, neck
- lower extremity: leg (knee and below), thigh, foot
- oral/genital: genitalia
- palms/soles: palms, soles
- posterior torso: back, buttock
- upper extremity: arm, forearm, hand

Supplementary Table 1. Histopathologically verified diagnosis across the technical domain (i.e. camera setup) and data source (i.e. hospital).

Technical Domain (TD)	Data Source	Non-melanoma	Melanoma
TD1	Hospital 1	322	245
	Hospital 2	210	55
	Hospital 3	27	39
	Combined	559	339
TD2	Hospital 4	92	123
	Hospital 5	75	31
	Combined	167	154
TD3	Hospital 6	109	67
	Hospital 7	83	93
	Combined	192	160
TD4	Hospital 8	242	97
	Combined	242	97

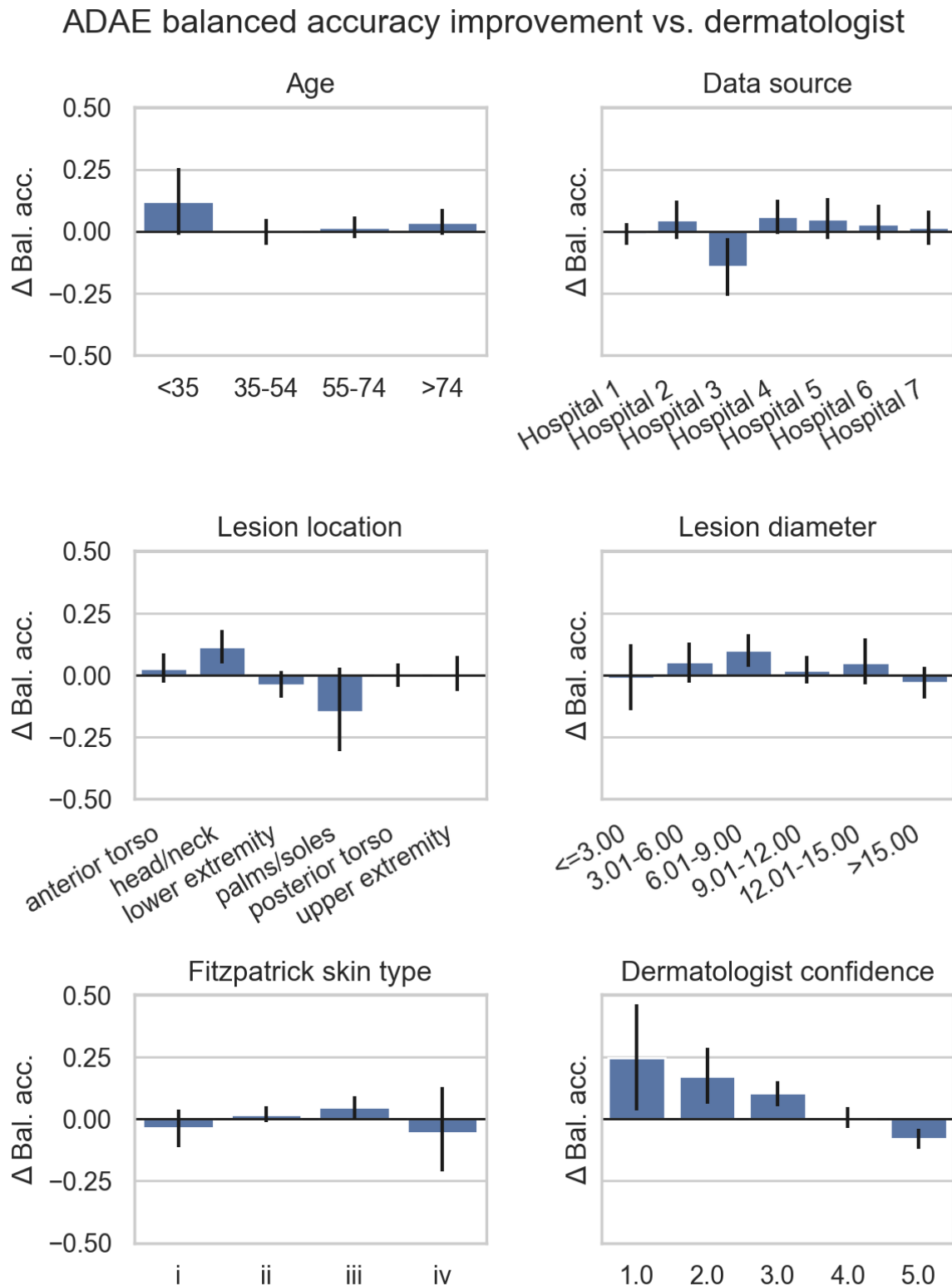
Supplementary Table 2. STARD 2015 Checklist.

Section and topic	No	Item	Section in manuscript
Title or abstract			
	1	Identification as a study of diagnostic accuracy using at least one measure of accuracy (such as sensitivity, specificity, predictive values or AUC)	Abstract
Abstract			
	2	Structured summary of study design, methods, results and conclusions	Abstract
Introduction			
	3	Scientific and clinical background, including the intended use and clinical role of the index test	Introduction
	4	Study objectives and hypotheses	Introduction
Methods			
Study design	5	Whether data collection was planned before the index test and reference standard were performed (prospective study) or after (retrospective study)	Study design
Participants	6	Eligibility criteria	Participants
	7	On what basis potentially eligible participants were identified (such as symptoms, results from previous tests, inclusion in registry)	Participants
	8	Where and when potentially eligible participants were identified (setting, location and dates)	Participants
	9	Whether participants formed a consecutive, random or convenience series	Participants
Test methods	10a	Index test, in sufficient detail to allow replication	Model Training and Testing Statistical Analysis
	10b	Reference standard, in sufficient detail to allow replication	Model Training and Testing Statistical Analysis

	11	Rationale for choosing the reference standard (if alternatives exist)	Model Training and Testing
	12a	Definition of and rationale for test positivity cut-offs or result categories of the index test, distinguishing prespecified from exploratory	Model Training and Testing
	12b	Definition of and rationale for test positivity cut-offs or result categories of the reference standard, distinguishing prespecified from exploratory	n.a.
	13a	Whether clinical information and reference standard results were available to the performers or readers of the index test	Study Design Model Training and Testing
	13b	Whether clinical information and index test results were available to the assessors of the reference standard	n.a.
Analysis	14	Methods for estimating or comparing measures of diagnostic accuracy	Statistical Analysis
	15	How indeterminate index test or reference standard results were handled	n.a.
	16	How missing data on the index test and reference standard were handled	Study Design Participants
	17	Any analyses of variability in diagnostic accuracy, distinguishing prespecified from exploratory	Statistical Analysis
	18	Intended sample size and how it was determined	Patient and Lesion characteristics Model Training and Testing
Results			
Participants	19	Flow of participants, using a diagram	n.a.
	20	Baseline demographic and clinical characteristics of participants	Patient and lesion characteristics
	21a	Distribution of severity of disease in those with the target condition	Patient and lesion characteristics
	21b	Distribution of alternative diagnoses in those without the target condition	Patient and lesion characteristics
	22	Time interval and any clinical interventions between index test and reference standard	n.a.
Test results	23	Cross tabulation of the index test results (or	Dermatologist versus

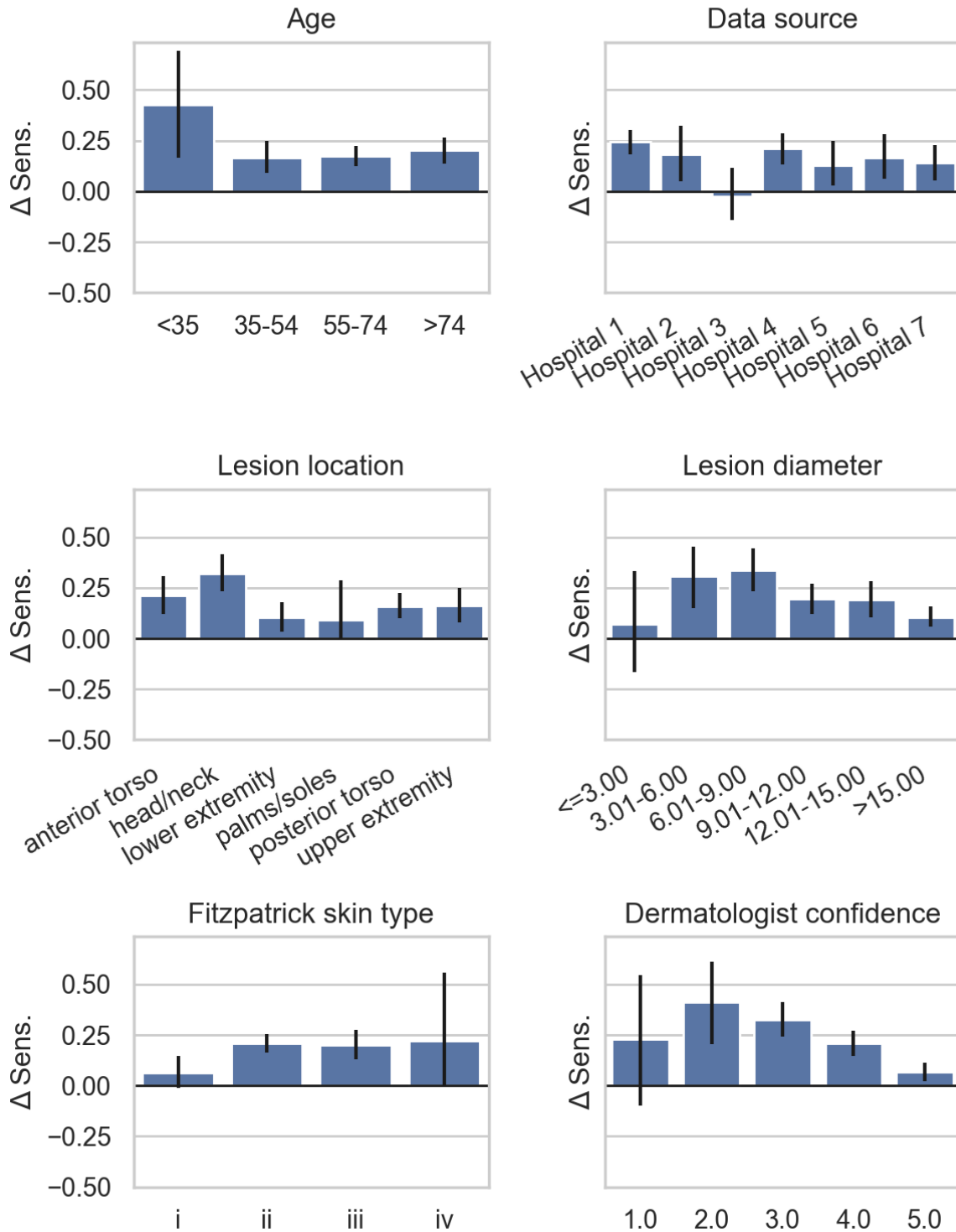
		their distribution) by the results of the reference standard	AI Performance impact of different variables
	24	Estimates of diagnostic accuracy and their precision (such as 95% CIs)	Dermatologist versus AI Performance impact of different variables
	25	Any adverse events from performing the index test or the reference standard	n.a.
Discussion			
	26	Study limitations, including sources of potential bias, statistical uncertainty and generalisability	Discussion
	27	Implications for practice, including the intended use and clinical role of the index test	Discussion
Other information			
	28	Registration number and name of registry	n.a.
	29	Where the full study protocol can be accessed	n.a.
	30	Sources of funding and other support; role of funders	Funding/Support Role of Funder/Sponsor

Supplementary Results



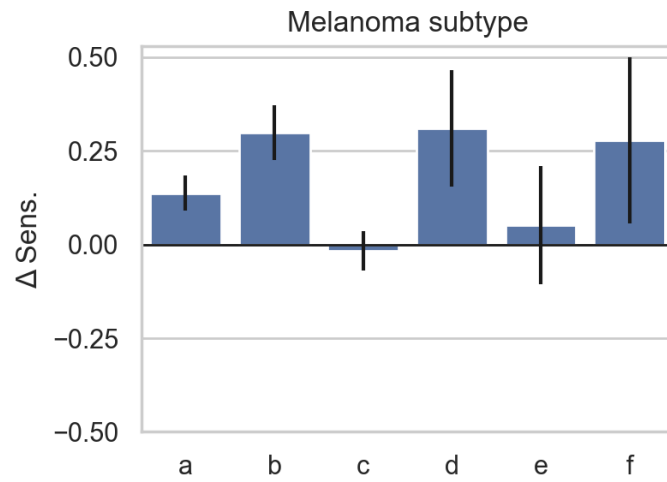
Supplementary Fig. 1. ADAE balanced accuracy improvements, stratified by patient age (top left), clinic (top right), lesion location (center left), lesion diameter (center right), patient Fitzpatrick skin type (bottom left), and dermatologist confidence (bottom right).

ADAE sensitivity improvement vs. dermatologist



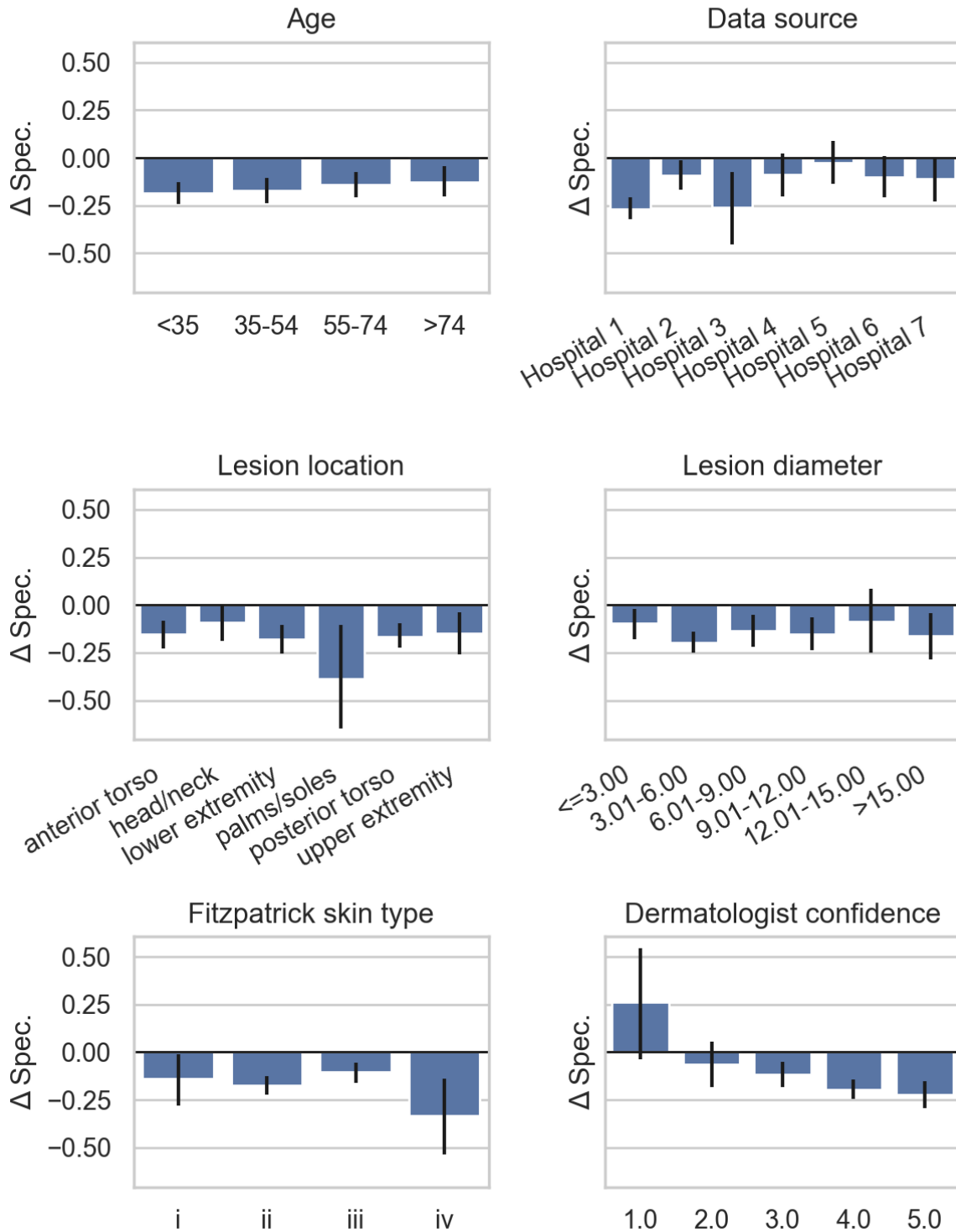
Supplementary Fig. 2. ADAE sensitivity improvements, stratified by patient age (top left), clinic (top right), lesion location (center left), lesion diameter (center right), patient Fitzpatrick skin type (bottom left), and dermatologist confidence (bottom right).

ADAE sensitivity improvement vs. dermatologist

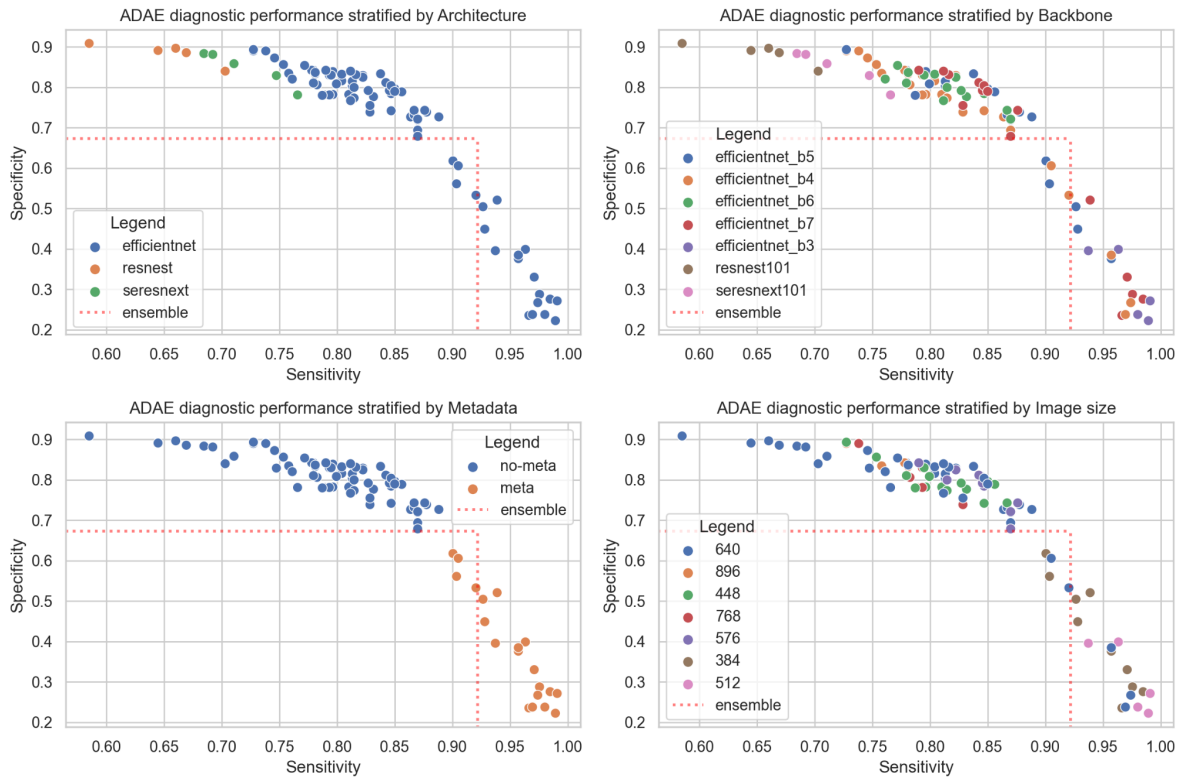


Supplementary Fig. 3. ADAE sensitivity improvements, stratified by Melanoma subtypes, a: superficial spreading, b: others, c: nodular, d: lentigo maligna, e: acral lentiginous, f: combined forms

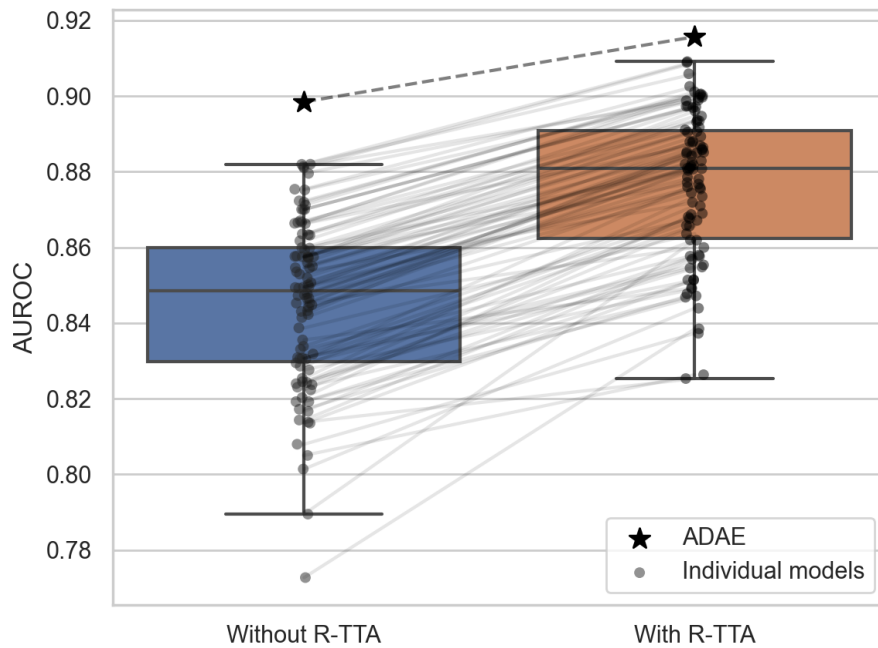
ADAE specificity improvement vs. dermatologist



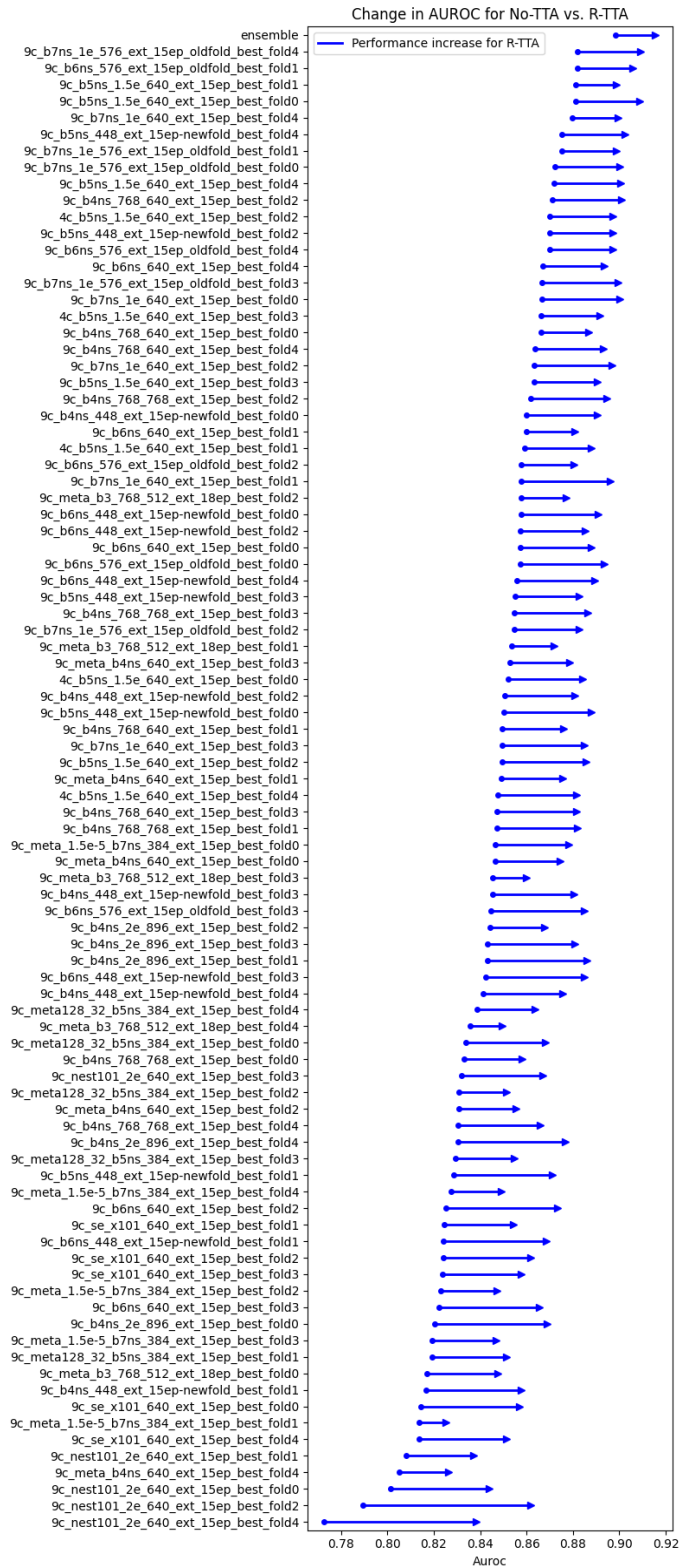
Supplementary Fig. 4. ADAE specificity improvements, stratified by patient age (top left), clinic (top right), lesion location (center left), lesion diameter (center right), patient Fitzpatrick skin type (bottom left), and dermatologist confidence (bottom right).



Supplementary Fig. 5. ADAE's diagnostic performance, stratified by architecture (top left), backbone (top right), metadata (bottom left), and image size (bottom right).

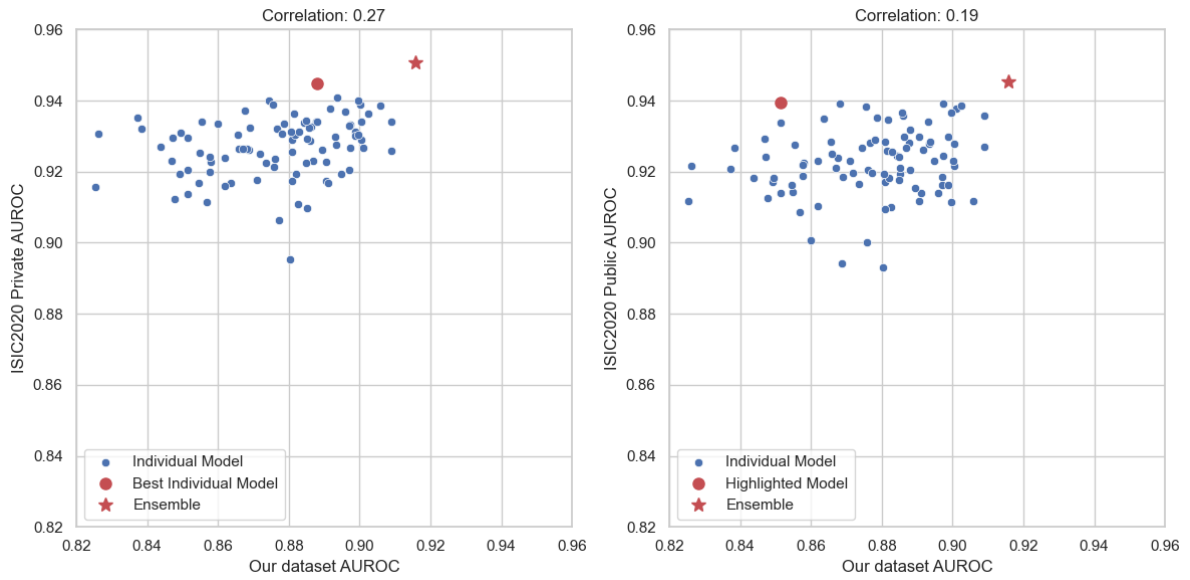


Supplementary Fig. 6. Impact of R-TTA: diagnostic accuracy of individual models. AUROC (diagnostic accuracy) of ADAE and its individual models with and without R-TTA. R-TTA: real test-time augmentation, AUROC: area under the receiver operating characteristic curve.



Supplementary Fig. 7. Impact of R-TTA: Change in diagnostic accuracy for individual models.

The change in AUROC (diagnostic accuracy) for each individual model and the ensemble itself when utilizing R-TTA. R-TTA: real test-time augmentation, AUROC: area under the receiver operating characteristic curve.



Supplementary Fig. 8: Correlation analysis. Correlation between the AUROC scores of the individual models of ADAE (without R-TTA) as well as the ensemble itself for ISIC 2020 test (left) and validation (right) set vs. our test set. AUROC: area under the receiver operating characteristic curve, R-TTA: real test-time augmentation